Heliyon 9 (2023) e20145

Contents lists available at ScienceDirect

Heliyon

journal homepage: www.cell.com/heliyon

Vine tea extract ameliorated acute liver injury by inhibiting hepatic autophagy and reversing abnormal bile acid metabolism

Ying Li [a,1], Ming-Wang Kong [a,1], Nan Jiang [c,d], Chen Ye [e], Xiao-Wei Yao [a], Xiao-Juan Zou [a], Hai-Ming Hu [b,**], Hong-Tao Liu [a,*]

[a] College of Basic Medical Sciences, Hubei University of Chinese Medicine, Huangjiahu West Road 16, Wuhan 430065, PR China
[b] School of Laboratory Medicine, Hubei University of Chinese Medicine, Huangjiahu West Road 16, Wuhan 430065, PR China
[c] Hubei Provincial Hospital of Traditional Chinese Medicine, Wuhan 430061, PR China
[d] Hubei Province Academy of Traditional Chinese Medicine, Wuhan 430074, PR China
[e] Wuhan Customs Technology Center, Qintai Avenue 588, Wuhan 430050, PR China

ARTICLE INFO

Keywords:
Liver fibrosis
Autophagosome
Intestinal metabolites
Vine tea
Gut microbiota

ABSTRACT

Gut microbiota disturbance, autophagy dysregulation, and accumulation of hepatic bile acids (BAs) are essential features of liver injury. Therefore, regulating autophagy and BA metabolism are potential strategies for treating liver diseases. Vine tea has been seen beyond a pleasant tea in food science. Our previous study found that vine tea extract (VTE) intervention alleviated acute liver injury (ALI) by restoring gut microbiota dysbiosis. In this study, we aim to investigate the effect of VTE on carbon tetrachloride (CCl_4)-induced hepatic autophagy and BA metabolism disorder in mice. The results showed that VTE effectively suppressed CCl_4-induced liver fibrosis and hepatic autophagy. LC-MS/MS assay suggested that VTE affected fecal BA production by reducing the fecal BA levels and improving cholestasis in ALI mice. Besides, VTE inhibited BA synthesis, promoted BA transport in the liver, and enhanced BA reabsorption in the ileum through the farnesoid X receptor (FXR)-related signaling pathway. The hepatic expressions of *Fxr* and *Abca1* were elevated by VTE. Finally, the depletion of gut microbiota in ALI mice had a negative impact on abnormal autophagy and BA metabolism. It was also noted that the administration of VTE did not provide any additional improvement in this regard. Overall, VTE ameliorated ALI by reversing hepatic autophagy and abnormal BA metabolism, and the beneficial effects of VTE on liver injury depended on the existence of gut microbiota.

1. Introduction

The liver is a vital organ with multiple functions, such as producing bile acids (BAs), maintaining glucolipid homeostasis, and metabolizing endogenous or xenobiotic toxins [1]. Acute liver injury (ALI), characterized by the rapid destruction of liver function with multiple organ failures, is a life-threatening syndrome with a mortality rate approaching 80% [2,3]. Risk factors for ALI include mitochondrial oxidative stress, autophagy, sterile inflammation, endoplasmic reticulum stress, and microcirculation dysfunction [4].

* Corresponding author.
** Corresponding author.
E-mail addresses: huhm1012@hbtcm.edu.cn (H.-M. Hu), hongtaoliu@hbtcm.edu.cn (H.-T. Liu).
[1] These authors contributed equally to this work.

https://doi.org/10.1016/j.heliyon.2023.e20145
Received 17 June 2023; Received in revised form 8 September 2023; Accepted 13 September 2023
Available online 14 September 2023

BAs, a class of amphiphilic molecules, are synthesized by the liver using cholesterol. Under physiological conditions, BAs are vital to promoting the digestion and absorption of lipids, inhibiting cholesterol precipitation in bile, regulating glycolipid metabolism, and activating immune responses [5,6]. However, excessive bile synthesis or impaired bile flow can cause cholestasis, trigger inflammation and liver damage [7]. For instance, ALI will disturb BA metabolism in the liver, resulting in cholestasis [8].

Autophagy plays a vital role in the development of various liver diseases. When the ALI occurs, hepatocyte autophagy is rapidly activated, causing mitochondrial damage, inflammation, and fibrosis in the liver [9,10]. With the progression of ALI, hepatic autophagy will be gradually inactivated, followed by increased oxidative stress, lipid peroxide accumulation, and the development of chronic liver diseases [11–13]. BAs can maintain liver function by regulating autophagy. In a recent study, the BA levels increased in the mouse liver after the knockout of nuclear factor farnesoid X receptor (FXR), accompanied by the activated hepatic autophagy [14]. In addition, some BAs can regulate the intestinal flora composition and protect gut barrier from damage by inhibiting the growth of "harmful bacteria" [15]. To date, there was no reports about the interaction between gut microbiota, BA metabolism and autophagy in the development of ALI.

Specific chemical reagents, namely Carbon tetrachloride (CCl_4), D-galactosamine (D-gal), and alcohol, are typically utilized to create the ALI animal model [16–18]. Among them, CCl_4 treatment leads to severe damage to the mouse liver, such as hepatomegaly, liver congestion, hepatocyte edema, and necrosis. These symptoms resemble acute chemical liver injury in humans [19]. Within the

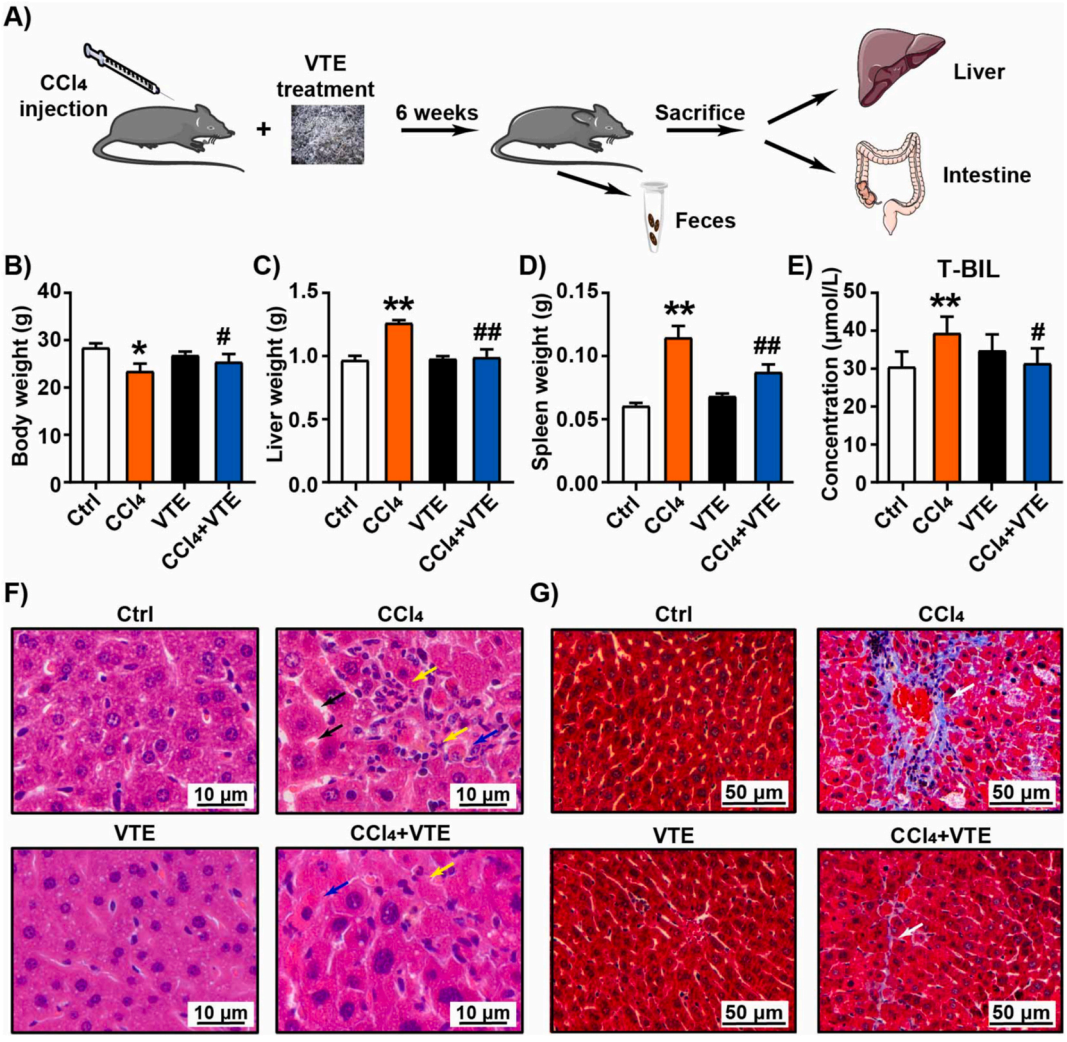

Fig. 1. Effect of VTE on physiological parameters and hepatic damage in ALI mice. (A) Schematic diagram of this study. To assess the effect of VTE on liver injury, we intraperitoneally injected C57BL/6J mice with CCl_4 twice a week for six weeks to establish an ALI murine model. Meanwhile, the mice were treated with VTE for six weeks. (B) Body weight change. (C) Liver weight change. (D) Spleen weight change. (E) Determination of T-BIL level in the liver. (F–G) Histopathological assay of liver tissues by H&E staining (F) (scale bar = 10 μm, magnification of the microphotograph, × 400) and Masson staining (G) (scale bar = 50 μm, magnification of the microphotograph, × 200). Black arrows indicate cellular edema. Blue arrows indicate eosinophilic transformation. Yellow arrows indicate cellular necrosis. White arrows indicate liver fibrosis. Data were presented as mean ± SEM. $^{*}p < 0.05$, $^{**}p < 0.01$ *vs.* Ctrl group; $^{\#}p < 0.05$, $^{\#\#}p < 0.01$ *vs.* CCl_4 group.

liver, CCl_4 is metabolized by the cytochrome P450 enzyme system into highly reactive trichloromethyl free radicals (•CCl3) and then to trichloromethyl peroxy radicals (•OOCCl3), which activates macrophages to produce pro-inflammatory cytokines [20]. The active free radicals attack polyunsaturated fatty acids in cellular membranes, leading to the peroxidation of lipids [21]. In addition, the CCl_4-generated ALI animal model is advantageous due to its simple operation and good repeatability. It is widely used to evaluate the protective effect of natural compounds against ALI [22]. In a prior study, we confirmed that CCl_4 administration resulted in liver inflammation, necrosis, and fibrosis in mice, replicating the ALI model [23].

Vine tea is made from the leaves of *Ampelopsis grossedentata,* a plant of the Vitis family. As a famous traditional Chinese tea, vine tea exhibits multiple biological activities, such as anti-inflammation, liver protection, anti-bacteria, blood lipid regulation, and anti-type 2 diabetes [24–28]. Vine tea contains various phytochemicals such as flavonoids, polyphenols, and terpenoids. Vine tea contains two primary bioactive compounds: dihydromyricetin and myricetin [29]. In mice models, studies have shown that dihydromyricetin and myricetin can inhibit the progression of hepatic fibrosis caused by CCl_4 [30,31]. In a previous study, we have discovered that vine tea extract (VTE) mainly consists of six components, including dihydromyricetin, quercetin 3-rhamnoside, myricetin, kaempferol, (−)-epicatechin gallate, and myricitrin [23]. And VTE could improve CCl_4-induced hepatocyte edema, inflammation, and necrosis [23]. In addition, VTE inhibits the growth of harmful bacteria, like *Intestinimonas*, *Alistipes*, and *Ruminiclostridium*, while promoting the colonization of potentially beneficial intestinal bacteria, such as *Ruminococcaceae_UCG-014* and *Eubacterium_fissicatena_group* [23]. However, it remains unclear about the regulation of BA metabolism and autophagy by VTE during the development of ALI.

In this study, based on a CCl_4-induced mouse ALI model, we explored the effect of VTE on hepatic autophagy and cholestasis in ALI mice. To determine whether VTE alleviated ALI by regulating BA metabolism, we determined the alteration of individual BAs in mouse feces. Further, we examined the expression changes in BA metabolism-related mediators in the liver and colon tissues of ALI mice after VTE treatment. Finally, we investigated the interaction between gut microbiota, BA metabolism, and hepatic autophagy in ALI mice.

2. Results

2.1. VTE improved liver fibrosis in ALI mice

Schematic diagram of this study was shown in Fig. 1A. As depicted in Fig. 1B, the body weight of mice in the CCl_4 group was decreased compared to that of the Ctrl group ($p < 0.05$), which was statistically reversed by VTE treatment ($p < 0.05$, *vs.* CCl_4 group). In addition, the liver and spleen weight in the CCl_4 group was increased ($p < 0.01$, *vs.* Ctrl group) (Fig. 1C and D). Interestingly, VTE suppressed the growth of both organs in ALI mice ($p < 0.01$, *vs.* CCl_4 group) (Fig. 1C and D). Also, VTE treatment significantly reduced the hepatic T-BIL level in ALI mice ($p < 0.05$, *vs.* CCl_4 group) (Fig. 1E). H&E staining indicated that VTE treatment ameliorated CCl_4-induced hepatocyte edema, eosinophilic transformation, and necrosis. H&E staining showed that CCl_4 induced significant liver damage, characterized by hepatocyte edema, eosinophilic transformation, and necrosis (Fig. 1F). As compared to the CCl_4 group, VTE intervention improved chronic liver injury and necrosis (Fig. 1F). Moreover, Masson staining demonstrated that VTE effectively suppressed CCl_4-induced liver fibrosis (Fig. 1G).

2.2. VTE alleviated CCl_4-induced autophagy

Since the autophagy signaling pathway is known to regulate liver injury, we investigated the effect of VTE on autophagy in the

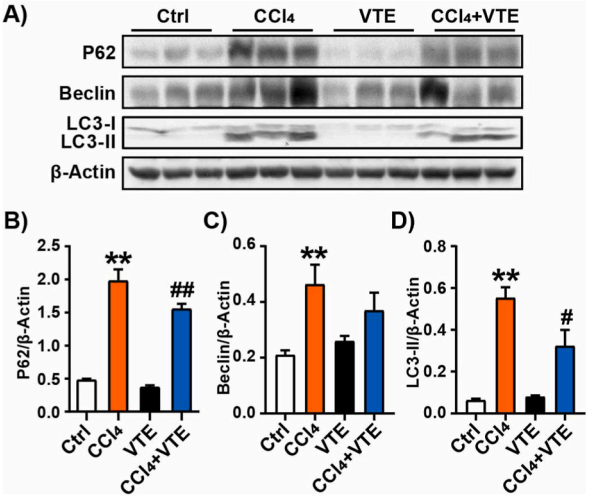

Fig. 2. Effect of VTE on protein levels of autophagic markers in liver of ALI mice. (A) Protein levels of autophagic markers in the liver by WB. The full images of blots were provided in Supplementary Figs. 2A–D. (B–D) Protein quantification of autophagic markers, including p62 (B), Beclin (C), and LC3-II (D). Data were presented as mean ± SEM. $^{*}p < 0.05$, $^{**}p < 0.01$ *vs* Ctrl group; $^{\#}p < 0.05$, $^{\#\#}p < 0.01$ *vs* CCl_4 group.

livers of ALI mice. Light chain 3 (LC3)-II is present on autophagosome membranes and disappears with the progression of autophagy [32]. Conversely, the autophagosome adaptor protein, p62/SQSTM1, is a mediator required for complete recruitment of microtubule-associated protein LC3 to the damaged lysosome [33]. Hence, we examined the protein changes of LC3I/II and p62 in the liver of ALI mice. As shown in Fig. 2A, B and D the hepatic levels of LC3-II and p62 were upregulated in the CCl_4 group ($p < 0.01$, *vs.* Ctrl group), which were statistically inhibited by VTE ($p < 0.05$ or $p < 0.01$, *vs.* CCl_4 group). Similarly, the level of Beclin was increased in the CCl_4 group ($p < 0.01$, *vs.* Ctrl group), but VTE treatment reverted such a change (Fig. 2A and C).

2.3. VTE affected fecal BA production in ALI mice

ALI is often accompanied by BA metabolism disorders, which are essential in mediating the development of hepatocyte autophagy [34]. Thus, we quantified the contents of intestinal metabolites among experimental groups by LC/GC-MS analysis. As shown in Fig. 3A and B, VTE reduced the levels of total BAs and secondary BAs in the feces of ALI mice ($p < 0.05$ or 0.01, *vs.* CCl_4 group). Compared with the Ctrl group, there was a higher tauro-murocholicacid (TMCA)/taurocholic acid (TCA) ratio in the CCl_4 group ($p < 0.05$) (Fig. 3C), which was statistically decreased in ALI mice with VTE treatment ($p < 0.01$, *vs.* CCl_4 group) (Fig. 3C). Additionally, the levels of deoxycholic acid (DCA), taurochenodeoxycholic acid (TCDCA), and ursodeoxycholic acid (UDCA) were elevated in feces of the CCl_4 group ($p < 0.05$ or 0.01, *vs.* Ctrl group), while the contents of cholic acid (CA), taurodeoxycholic acid (TDCA), and tauroursodeoxycholic acid (TUDCA) were reduced ($p < 0.05$ or 0.01, *vs.* Ctrl group) (Fig. 3D). However, VTE treatment significantly reversed such changes in ALI mice ($p < 0.05$ or 0.01, *vs.* CCl_4 group) (Fig. 3D).

2.4. VTE suppressed changes of BA synthesis and transportation in ALI mice

Next, we examined the effect of VTE on BA synthesis in the liver of ALI mice. By qRT-PCR, we detected the mRNA levels of BAs metabolism-related genes in liver or colon tissues among the four experimental groups. First, we tested the genes responsible for BA synthesis. As illustrated in Fig. 4A–D, the expressions of *Cyp7a1* and *Cyp2c70* were increased in liver tissues of the CCl_4 group ($p < 0.05$ or 0.01, *vs.* Ctrl group), whereas *Cyp8b1* and *Cyp27a1* were decreased ($p < 0.05$ or 0.01, *vs.* Ctrl group). On the contrary, these altered

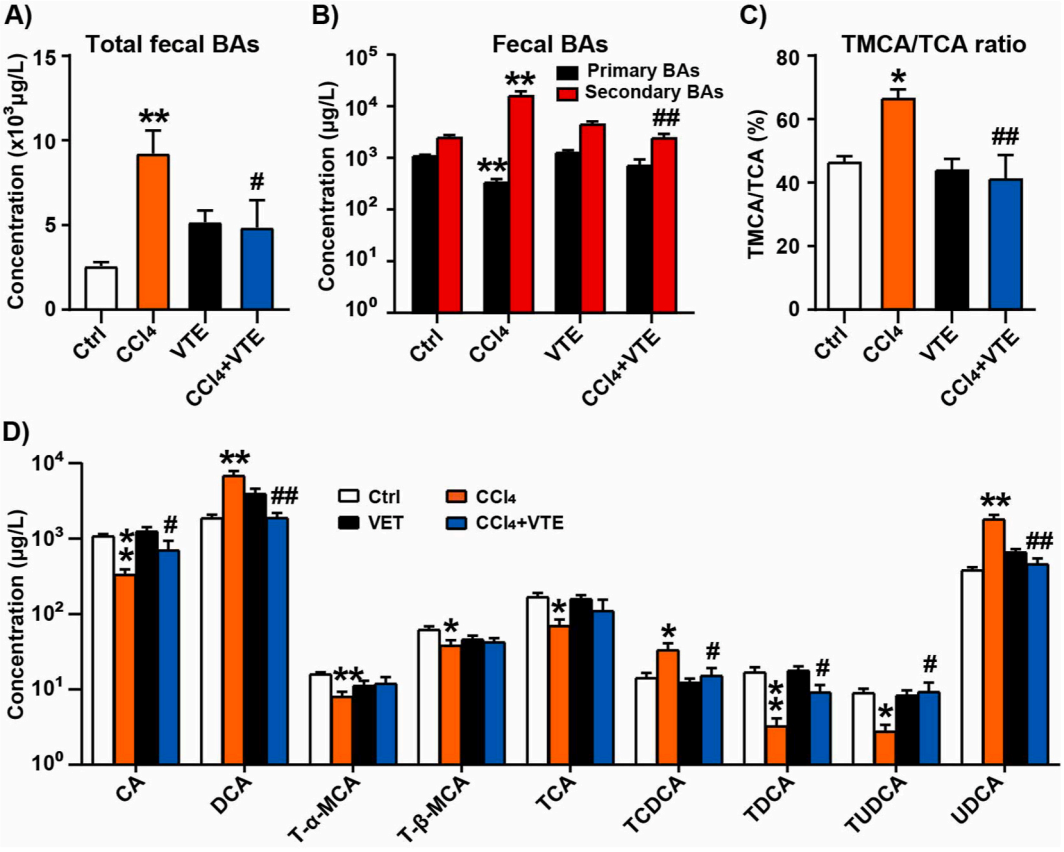

Fig. 3. Effect of VTE on production of fecal BAs in ALI mice. (A) Contents of total fecal BAs among four experimental groups. (B) Levels of primary and secondary BAs in feces. (C) Ratio of TMCA/TCA. (D) Quantitative analysis of individual BAs in feces. Data were presented as mean ± SEM. $^{*}p < 0.05$, $^{**}p < 0.01$ *vs* Ctrl group; $^{\#}p < 0.05$, $^{\#\#}p < 0.01$ *vs* CCl_4 group.

BA synthetases were significantly restores in ALI mice with VTE treatment ($p < 0.01$, *vs.* CCl_4 group) (Fig. 4A–D). Second, we detected the mRNA expressions of genes responsible for transport or feedback regulation of BAs in the liver and colon. The result showed that the mRNA levels of hepatic *Lxr*, *Fxr*, and *Abca1* were lower and the mRNA levels of hepatic *Ntcp* were higher in the CCl_4 group than in the Ctrl group. Conversely, the hepatic expressions of *Fxr* and *Abca1* were statistically elevated and the hepatic expressions of *Ntcp* were increased by VTE in ALI mice ($p < 0.05$ or 0.01, *vs.* CCl_4 group) (Fig. 4 E–H). In parallel, CCl_4 injection caused the decrease in mRNA levels of *Fxr* and *Asbt* in the colon ($p < 0.05$ or 0.01, *vs.* Ctrl group), whereas VTE blocked the changes of both genes in ALI mice ($p < 0.05$, *vs.* CCl_4 group) (Fig. 4I and J).

Furthermore, we performed Spearman's correlation analysis, indicative of a heat map (Fig. 4K). The result suggested that most of the altered autophagy markers, BAs, BA synthesis, BA transport, and BA feedback regulation were positively or negatively associated with physiological and pathological ALI markers, indicating the pivotal role of autophagy and BA metabolism in the participation of ALI.

2.5. *VTE failed to ameliorate liver injury and hepatic autophagy in ALI mice with gut microbiota depletion*

To examine the role of gut microbiota in VTE-mediated prevention of liver injury, we pretreated mice with an antibiotic mixture to remove intestinal bacteria before the administration of CCl_4 and VTE (Fig. 5A, Supplementary Fig. 1). The result indicated that Abx treatment had no effect on the body weight but remarkably decreased the weight of liver and spleen tissues in ALI mice ($p < 0.01$ *vs.*

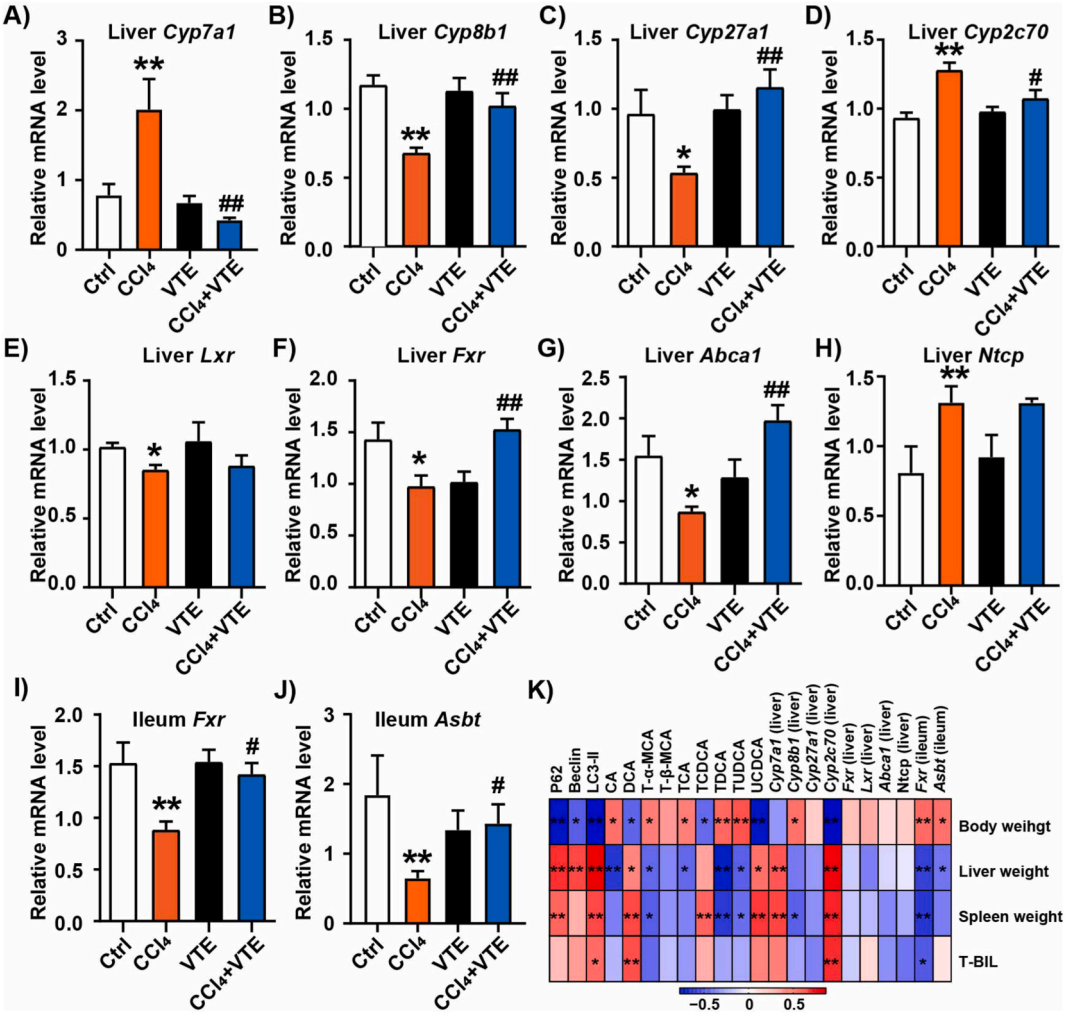

Fig. 4. Effect of VTE on BA metabolism in ALI mice and correlation analysis between BA metabolism and autophagy. (A–D) mRNA levels of BA synthesis-related genes in the liver by qRT-PCR, including *Cyp7a1* (A), *Cyp8b1* (B), *Cyp27a1* (C), and *Cyp2c70* (D). (E–H) mRNA levels of genes responsible for feedback regulation and transport of BAs in the liver by qRT-PCR, including *Lxr* (E), *Fxr* (F), *Abca1*(G), and *Ntcp* (H). (I–J) mRNA levels of BA transport-related genes in the ileum by qRT-PCR, including *Fxr* (I) and *Asbt* (J). Data were presented as mean ± SEM. $^{*}p < 0.05$, $^{**}p < 0.01$ *vs* Ctrl group; $^{\#}p < 0.05$, $^{\#\#}p < 0.01$ *vs* CCl_4 group. (K) Spearman's correlation analysis between BAs, BA metabolism-related genes, and autophagic markers was calculated in the heatmap. $^{*}p < 0.05$, $^{**}p < 0.01$.

CCl_4 group), which were not further improved after VTE treatment (Fig. 5B–D). Besides, VTE failed to ameliorate hepatocyte necrosis and inflammation in mice of the CCl_4 + Abx and ACl_4 + Abx + VTE group (Fig. 5E).

Next, we detected the effect of VTE on autophagy in ALI mice with gut microbiota depletion. As indicated in Fig. 5F and G, CCl_4 administration led to the protein increase in hepatic autopay markers, including p62, Beclin, and LC3-II ($p < 0.05$ or 0.01 *vs.* Ctrl group). Compared to the CCl_4 group, Abx had no effect on p62, Beclin, and LC3-II (Fig. 5F and G). At the same time, we found no expression differences in these proteins between the CCl_4 +Abx and CCl_4 + Abx + VTE groups (Fig. 5F and G).

2.6. VTE failed to alleviate abnormal BA metabolism in ALI mice with gut microbiota depletion

Finally, we detected the effect of VTE on BA metabolism in ALI mice with gut microbiota depletion. As suggested in Fig. 6, VTE did not rescue the abnormal BA metabolism of ALI mice after the gut microbiota was destructed by an antibiotic mixture (Fig. 6). Similar to the results in Fig. 4, the CCl_4 group displayed higher mRNA levels of hepatic *Cyp7a1*, *Cyp2c70*, and *Ntcp* and lower levels of *Cyp8b1*, *Cyp27a1*, *Lxr*, *Fxr*, and *Abca1* ($p < 0.05$ or 0.01, *vs.* Ctrl group) (Fig. 6A–H). Also, CCl_4 treatment reduced the intestinal mRNA levels of *Fxr* and *Asbt* ($p < 0.05$, *vs.* Ctrl group) (Fig. 6I and J). However, either Abx or Abx + VTE failed to rescue these changes in ALI mice, except for the hepatic mRNA levels of *Ntcp* (Fig. 6).

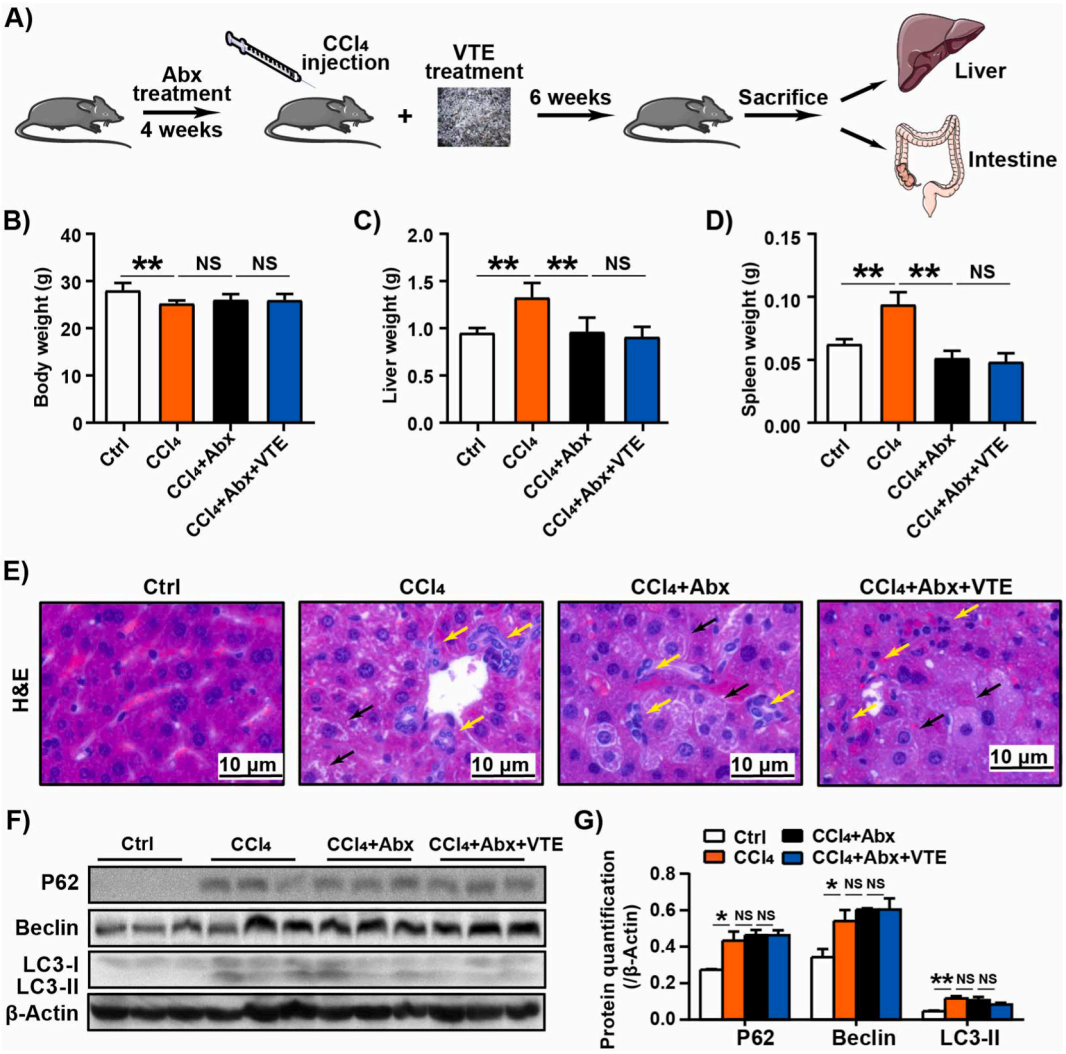

Fig. 5. Effect of VTE on liver damage in ALI mice with gut microbiota depletion. (A) Schematic diagram that shows effect of VTE on ALI mice with gut microbiota depletion. (B) Body weight change. (C) Liver weight change. (D) Spleen weight change. (E) Histopathological assay of liver tissues by H&E staining (scale bar = 10 μm, magnification of the microphotograph, × 400). Black arrows indicate cellular edema, and yellow arrows indicate cellular necrosis. (F) Protein levels of autophagic markers in the liver by WB. The full images of blots were provided in Supplementary Figs. 2E–H. (G) Protein quantification of autophagic markers, including p62, Beclin, and LC3-II. Data were presented as mean ± SEM. *$p < 0.05$, **$p < 0.01$. NS, no significance.

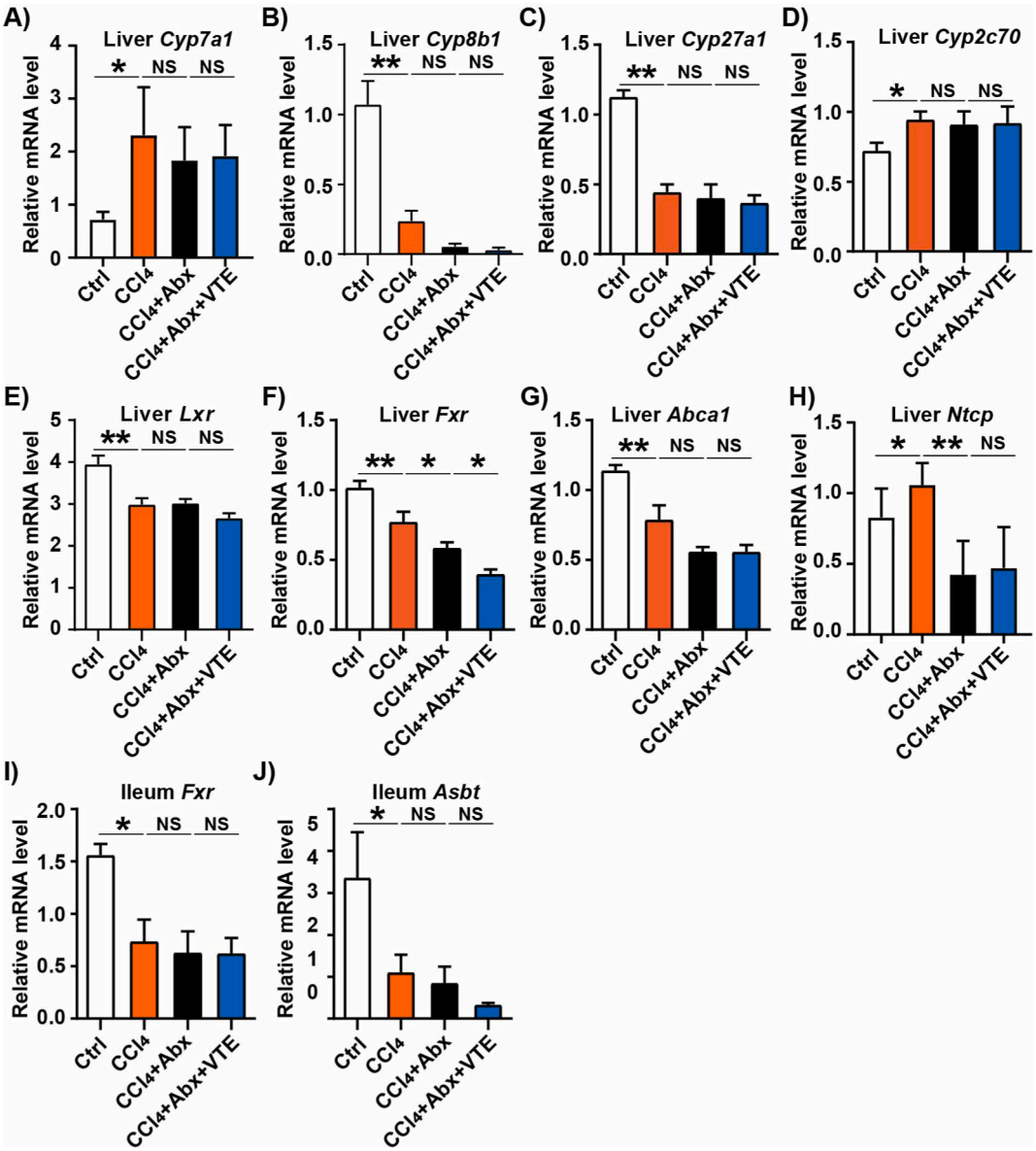

Fig. 6. Effect of VTE on mRNA expression of BA metabolism-related mediators in liver and gut of ALI mice with gut microbiota depletion. (A–D) mRNA expression of genes involved in BA synthesis in the liver by qRT-PCR, including *Cyp7a1* (A), *Cyp8b1*(B), *Cyp27a1*(C), and *Cyp2c70* (D). (E–H) mRNA expression of genes involved in BA feedback regulation and transport in the liver by qRT-PCR, including *Lxr* (E), *Fxr* (F), *Abca1*(G), and *Ntcp* (H). (I–J) mRNA expression of *Fxr* (I) and *Asbt* (J) genes in the gut by qRT-PCR. Data were presented as mean ± SEM. $^{*}p < 0.05$, $^{**}p < 0.01$. NS, no significance.

3. Discussion

Applying BA sequestrants, gut probiotics, and medicinal plants is a potential strategy for treating liver diseases [8,35–37]. For instance, Sevelamer, a BA chelator, could prevent non-alcoholic steatohepatitis by modulating gut microbiota structure and BA composition [8]. Many herbs or ingredients are well-studied for their hepatoprotective activity [38,39]. Curcumin supplementation could be a nutritional approach to prevent hepatic cellular senescence [40]. Liu et al. reported that oral administration with *Lactobacillus rhamnosus GG* ameliorated liver fibrosis in mice through the intestinal FXR–fibroblast growth factor (FGF)-15 signaling pathway, which inhibits hepatic BA synthesis and enhanced BA excretion [35]. In addition, some medicinal plant extracts, like baicalein and dihydromyricetin, relieved cholestasis and liver fibrosis by modulating BA metabolism and gut microbiota structure [36,37]. In this study, VTE exhibited a protective effect on CCl_4-induced ALI in mice by alleviating gut dysbiosis, regulating BA metabolism, and inhibiting hepatic autophagy.

Autophagy is a highly conserved cyclic process involving the cytosolic degradation of intracellular proteins and damaged organelles [12]. Studies show that autophagy is impaired in hepatocytes of mice with NAFLD and non-alcoholic steatohepatitis (NASH) [41,42]. Among the autophagic indicators, the LC3-II amount is correlated with the number of autophagosomes [43], which are essential for phagosome expansion [32]. And p62 is a mediator necessary for LC3 recruitment to lysosomes, vital for the selective degradation of autophagy substrates [33,44]. The p62 binding to LC3 is essential for autophagosome clearance [44]. In the liver, accumulation of p62 can raise autophagosome accumulation, leading to cytotoxic effects and aggravating liver injury [34]. Increased LC3-II and p62-positive aggregates were found in the liver of patients with primary biliary cirrhosis [45]. Therefore, this study selected LC3-II and p62 as markers to analyze the initiation and degradation of autophagy. Our data indicate that CCl_4 induced the increment of LC3-II and p62 proteins in the mouse liver (Fig. 2), implying the occurrence of hepatic autophagy. However, VTE treatment significantly suppressed the up-regulation of LC3-II and p62 in the liver of ALI mice. These results suggest that VTE may play a protective role in the liver by inhibiting the accumulation of autophagosomes. Still, the precise autophagy dynamics that ensue after VTE treatment are required for further investigation.

As we discovered in our previous study, VTE is primarily composed of six key components: dihydromyricetin, quercetin 3-rhamnoside, myricetin, kaempferol, (−)-epicatechin gallate, and myricitrin [23]. Several main components of vine tea, such as dihydromyricetin, myricetin, and (−)-epicatechin gallate, have been reported to regulate autophagy. One example is dihydromyricetin, which plays a protective role in H9C2 cells by inhibiting autophagy and cell apoptosis [46]. Additionally, the combination of myricetin and cucurbitacin E exited anti-cancer activity, and the mechanism is related to the inhibition of autophagy and the activation of the PI3K/AKT/mTOR signaling pathway [47]. In another study, (−)-epicatechin gallate downregulated autophagy by modulating the PI3K/AKT/mTOR pathway [48]. Based on the above, the major compounds of VTE, like dihydromyricetin, myricetin, and (−)-epicatechin gallate, may play an essential role in regulating abnormal autophagy in ALI mice.

We next investigated other factors that might trigger the abnormal accumulation of hepatic autophagosomes in ALI mice. Since the literature confirmed that BAs could regulate hepatic autophagy through various mechanisms [49,50], we focused our research on the changes in BA metabolism after VTE treatment. The result shows that CCl_4 injection led to increased levels of total and secondary BAs in mouse feces, which were reversed by VTE treatment (Fig. 3A and B). Considering that intestinal BAs come from the bile, followed by subsequent reabsorption into the liver, we speculate that VTE may ameliorate the abnormal BA metabolism by regulating hepatic BA synthesis or promoting colonic BA transport into the liver. Indeed, VTE treatment significantly repressed the alteration of BA metabolism-related mediators in ALI mice (Fig. 4). These mediators were mainly responsible for BAs' synthesis, transport, and feedback regulation. Among them, FXR is a BA-specific receptor in the liver and gut. FXR activation reduces intracellular BA load in the liver via inhibiting BA synthetases (i.e., CYP7A1), suppressing BA reabsorption transporters (i.e., NTCP and ASBT), and increasing BA export pump expressions (i.e., bile salt export pump (BSEP) organic solute transporter alpha-beta (OSTα/β)) [51]. In this study, VTE treatment statistically elevated the *Fxr* mRNA level in the liver and intestine of ALI mice (Fig. 4F and I). In addition, the increase in TMCA/TCA ratio can inhibit the expression of FXR [34]. In this study, VTE treatment statistically reduced the fecal TMCA/TCA ratio (Fig. 3C), further proving the role of BAs in VTE-initiated promotion of *Fxr* expression. On the other hand, BAs travel through the bile ducts to the duodenum and then are reabsorbed from the gut by specific BA transporters like (ASBT). Thus, the inhibition of ASBT can block the enterohepatic circulation of BAs [33]. We found that VTE intervention significantly increased the expression of *Asbt* in the gut of ALI mice (Fig. 4J). These results suggest that VTE might ameliorate liver injury by elevating FXR expression, inhibiting BA synthesis, and promoting BA reabsorption in the gut.

BAs regulate hepatocyte autophagy by activating inflammation and apoptosis signaling pathways [49,52]. In a previous study, the bile in mice lacking autophagy-related genes (Atg7 or Atg5) in the liver exhibited a decrease in secondary BAs and an increase in T-α-MCA and T-β-MCA [34]. In parallel, we found that VTE suppressed secondary BAs and slightly increased the above two free BAs (Fig. 3B and D), suggesting that VTE may improve BA metabolism by inhibiting hepatic autophagy in ALI mice. Additionally, DCA is generally considered a toxic BA that can induce inflammation and activate autophagy [50]. In the present study, CCl_4 treatment raised the fecal DCA concentration in mice. Conversely, VTE treatment markedly reduced the content of DCA (Fig. 3D), confirming that VTE may hamper autophagy by improving BA metabolism.

Gut microbiota contributes to BA metabolism and recycling [53,54]. In the ileum and colon, intestinal bacteria transform primary BAs into secondary BAs. Besides, gut microbes like *B. dentium* are closely related to autophagy [55]. It was reported that *B. dentium* can promote autophagy and release mucin granules stored in intestinal goblet cells [55]. Based on the germ-free ALI mouse model, we evaluated the effect of VTE on hepatic autophagy and bile acid metabolism. We found that after the intestinal flora was cleared by antibiotics, VTE no longer suppressed the hepatic autophagy, indicated by the unchanged autophagic markers in the mouse liver (Fig. 5). Moreover, VTE failed to improve the abnormal synthesis and transportation of BAs in ALI mice with gut microbiota depletion (Fig. 6). Taken together, the regulatory effect of VTE on hepatic autophagy and BA metabolism in ALI mice depends on the existence of their intestinal flora.

Several main components of vine tea, such as dihydromyricetin, quercetin, and kaempferol, have been documented to regulate BA metabolism. For instance, dihydromyricetin administration enhanced the BA conjugation and transport in the liver but inhibited BA reabsorption in the ileum through the FXR-related signaling pathway to prevent obesity [56]. Quercetin enhanced hepatic expression of BA synthesis- and transport-related genes in NAFLD mice [57]. In another study, kaempferol may promote BA transport by increasing the hepatic CYP27A1 and NTCP expression in NASH mice [58]. Based on the above, we speculate that the above components of VTE may play a direct role in regulating BA metabolism in ALI mice.

Our previous research has studied the abundance and composition of intestinal flora in ALI mice [23]. CCl_4 down-regulated the abundances of Lachnospiraceae, Bacteroidales_S24-7_group, and Staphylococcaceae. In contrast, CCl_4 augmented the contents of Ruminococcaceae, Streptococcaceae, and Anaeroplasmataceae. Noticeably, VTE treatment reversed these changes. For example, VTE

intervention inhibited the growth of harmful bacteria, like *Intestinimonas*, *Alistipes*, and *Ruminiclostridium*, while promoting the colonization of potentially beneficial intestinal bacteria, such as *Ruminococcaceae_UCG-014* and *Eubacterium_fissicatena_group* [23]. In this study, we focus on investigating the impact of VTE on hepatic autophagy and cholestasis during the development of ALI. To achieve this, we selected representative species to detect gut microbiota composition in antibiotic-treated mice (Supplementary Fig. 1). In the future, we aim to refine our study by exploring the abundance of gut microbiota in mice after antibiotic administration.

However, the empirical results reported herein should be considered in light of some limitations. Although we reported for the first time that VTE could improve ALI through the two-way regulation of liver autophagy and bile acid metabolism, the key targets linking autophagy and bile acid need to be further explored. Second, this study found that intestinal flora may be an essential bridge between liver autophagy and bile acid metabolism. However, which bacteria play a vital role in this process still needs to be determined. Third, during our preliminary study, mice underwent six weeks of VTE treatment with no adverse reactions observed. Further research is required to assess the safety and efficacy of long-term supplements for VTE.

4. Conclusions

This study demonstrated that vine tea water extract (VTE) could alleviate liver injury in ALI mice by suppressing liver fibrosis and reversing cholestasis. The underlying mechanism of VTE was associated with the reversal of hepatic autophagy and abnormal BA metabolism, which depended on the existence of normal gut microbiota community (Fig. 7). These findings suggest beneficial effects of VTE on human health.

5. Materials and methods

5.1. Animal experiments

Healthy male C57BL/6J mice (four weeks old) were purchased from Hubei Provincial Center for Disease Control and Prevention (Wuhan, China). Mice were sheltered with free access to sterile water and standard food. After one week of acclimatization in a 12 h dark/light cycle with controlled temperature (23 ± 2 °C) and moisture (50 ± 5%), the mice were divided into four groups (n = 8): Ctrl group, CCl_4 group, VTE group, and CCl_4 + VTE group. Detailed information about the preparation and composition analysis of VTE was shown in our previous report [23]. In our initial study, we monitored the water intake of mice that were given VTE (1 mg/mL, dissolved in drinking water). Our findings revealed that each mouse consumed an average of 4–5 mL of VTE per day. The mice had an average weight of 20–25 g, and based on our calculations, the estimated daily VTE dosage for the mice was 200 mg/kg. And administering VTE to mice for six weeks did not result in negative reactions. Consequently, we selected this dosage to treat mice in our subsequent studies. For each group, the mice were pretreated with sterile water (Ctrl group and CCl_4 group) or VTE (1 mg/mL in drinking water, about 200 mg/kg/d) [23] (VTE group and CCl_4+VTE group) for six weeks. Meanwhile, the mice in the CCl_4 and CCl_4+VTE group received 12 consecutive intraperitoneal injections of CCl_4 (1 μL/g body weight, dissolved in olive oil, v/v, 1:2, Aladdin) twice per week. In comparison, the mice in the Ctrl and VTE groups received intraperitoneal injections of olive oil (3 μL/g

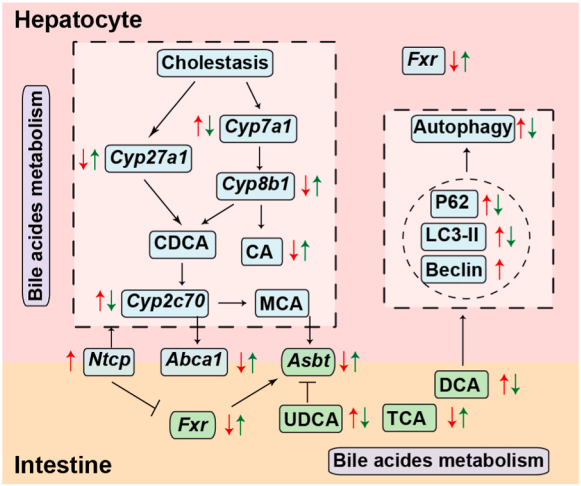

Fig. 7. Schematic diagram showing how VTE suppressed hepatic autophagy and improved bile acid (BA) metabolism in ALI mice. Firstly, VTE intervention decreased the levels of toxic BAs (like UDCA and DCA) but increased those of beneficial BAs, such as CA, T-α-MCA, T-β-MCA, and TCA. Secondly, VTE reduced hepatic cholestasis by inhibiting BA synthesis-related gene expressions (*Cyp7a1* and *Cyp2c70*), upregulating BA transport-related gene expressions (*Fxr* and *Abca1*), and promoting BA reabsorption-related gene expressions (*Fxr* and *Asbt*). Thirdly, VTE suppressed autophagic activation in the liver, as indicated by the down-regulation of autophagy markers (p62, Beclin, LC3-II). Red arrows indicate changes in the CCl_4 group compared to the Ctrl group; Green arrows indicate the changes in the VTE + CCl_4 group compared to the CCl_4 group.

body weight) (Fig. 1A).

For antibiotic treatment, mice were randomly divided into four groups (n = 8): Ctrl group, CCl_4 group, CCl_4 + Abx group, and CCl_4 + Abx + VTE group. The mice were treated with CCl_4 (1 μL/g body weight) twice per week, CCl_4 plus an antibiotic mixture (Abx, 1.0 mg/mL ampicillin, 0.5 mg/mL vancomycin, 1.0 mg/mL neomycin sulfate, and 0.5 mg/mL metronidazole, in drinking water), or CCl_4 plus Abx and VTE (200 mg/kg/d, gavage) (Fig. 6A). The antibiotic regimen used in this study was based on previous studies [59,60]. And after conducting several preliminary experiments, we found that this treatment effectively eliminates most microorganisms in mice's intestinal tract. This treatment plan has also been reported in multiple papers from our laboratory [61,62].

During the experiment, the body weight was monitored every week. For two consecutive days in the last week, the mice were placed in a metabolic cage to collect feces for 1 h, and the collected feces were stocked at −80 °C. After the treatment, all mice were euthanized, and the major tissues, including liver and intestine tissues, were collected and stored at −80 °C for further analysis. The animal experiment was performed under the local Ethical Committee (approval number: SYXK-2019-0067) and the National Act on Use of Experimental Animals (China).

5.2. Measurement of hepatic total bilirubin (T-BIL)

T-BIL in liver tissues was analyzed using a commercial kit from Changchun Huili Biotech Co., Ltd.

5.3. Histopathological analysis

Hepatic tissues were fixed overnight in 4% paraformaldehyde and then embedded in paraffin for sectioning. The morphological changes were determined using a hematoxylin-eosin (H&E) staining kit (Beyotime Biotechnology). The degree of liver fibrosis was detected using a Masson staining kit (ZhongHuiHeCai). The image was photographed with a Leica DFC310 FX digital camera attached to a Leica DMI4000B light microscope (Wetzlar).

5.4. Western blotting

Total proteins were extracted from liver tissues using RIPA buffer (Beyotime) supplemented with a protease inhibitor cocktail kit (Merck). The concentration of protein lysate was determined using a bicinchoninic acid (BCA) assay kit (Beyotime). Protein samples were separated by sodium dodecyl sulfate-polyacrylamide gel electrophoresis gels and electrophoretically transferred to polyvinylidene difluoride membranes. The membranes were blocked with 5% skim milk in Tris-buffered saline tween-20 (TBST) for 1 h, followed by incubation overnight at 4 °C with primary antibodies including rabbit anti-P62 (1:1000, Cell Signaling Technology), rabbit anti-Beclin (1:1000, Cell Signaling Technology), rabbit anti-LC3-II (1:1000, Cell Signaling Technology), mouse anti-β-Actin (1:500, Santa Cruz) antibodies. Then, the membranes were washed with TBST and incubated with horseradish peroxidase-conjugated secondary antibodies (1:5000, Cell Signaling Technology) at room temperature for 1 h. Immunoreactive bands were visualized by enhanced chemiluminescence solution (ECL, Cell Signaling Technology). β-Actin was used as a reference protein. All bands were analyzed using Image J2x software (National Institute of Health).

5.5. Fecal BA quantification by liquid chromatography-mass spectrometer (LC-MS)

To quantify the contents of BAs in feces, we homogenized a 50 mg fecal sample with 1 mL water-methanol-formic acid solution (25:74:1, V/V/V), containing 0.2 μg/mL cholic acid-2,2,3,4,4-d5 (d5-CA) and 0.2 μg/mL sodium taurocholate-2,2,4,4-d4 (d4-TCA) as internal standards. After the homogenization using a KZ-II grinding machine (Servicebio), we centrifuged the fecal mixtures at 12,000×*g* for 15 min at 4 °C. The supernatant was collected and filtered through a 0.22 μm water or organic membrane. After that, all samples were used for liquid chromatography-mass spectrometer (LC-MS) analysis. The detailed analytical information was indicated in the Supplementary methods.

5.6. Quantitative real-time reverse transcription PCR (qRT-PCR)

Total RNA from liver or colon tissues (~20 mg) was extracted using Trizol reagents (Summer Bio) according to the manufacturer's instructions. The cDNA was synthesized from 1 μg of total RNA with a first-strand cDNA synthesis kit (Summer Bio). We evaluated the mRNA levels of genes by qRT-PCR using the SYBR qPCR Mix (Summer Bio) on a Bio-Rad CFX Connect Real-time System (BioRad). The qRT-PCR was conducted as follows: initial denaturation at 95 °C for 10 min; 45 cycles of amplification (denaturation at 95 °C for 10 s, annealing at 60 °C for 30 s, and extension at 72 °C for 30 s), and extension at 95 °C for 5 min. The relative expression of each target gene was normalized to a reference gene *β-actin*, and calculated using the $2^{-\Delta\Delta CT}$ method. The primer sequences of target genes were detailed in Supplementary Table 1, including cytochrome p450 family 7 subfamily A member 1 (*Cyp7a1*), cytochrome p450 family 8 subfamily B member 1 (*Cyp8b1*), cytochrome p450 family 27 subfamily A member 1 (*Cyp27a1*), cytochrome p450 family 2 subfamily C member 70 (*Cyp2c70*), liver X receptor (*Lxr*), farnesoid X receptor (*Fxr*), ATP binding cassette transporter A1 (*Abca1*), sodium taurocholate cotransporting polypeptide (*Ntcp*) and apical sodium salt bile transporter (*Asbt*).

5.7. Statistical analysis

Results were presented as means ± standard error of the mean (SEM). Data were analyzed using GraphPad Prism (version 8.0, La Jolla). A two-way analysis of variance (ANOVA) was used to compare all groups where appropriate. Statistical significance was considered at a P value < 0.05.

Author contribution statement

Hongtao Liu: Conceived and designed the experiments; Wrote the paper.
Ying Li: Performed the experiments; Analyzed and interpreted the data; Wrote the paper.
Ming-Wang Kong; Nan Jiang; Xiao-Juan Zou: Performed the experiments; Contributed reagents, materials, analysis tools or data.
Chen Ye: Contributed reagents, materials, analysis tools or data.
Xiao-Wei Yao: Performed the experiments.
Hai-Ming Hu: Analyzed and interpreted the data; Wrote the paper.

Data availability statement

Data will be made available on request.

Declaration of competing interest

The authors declare that they have no known competing financial interests or personal relationships that could have appeared to influence the work reported in this paper.

Acknowledgements

This work was financially supported by Knowledge Innovation Program of Wuhan (NO. 2022020801010420), Health Commission of Hubei Province of China (NO. ZY2021M107), Department of Science and Technology of Hubei Province (NO. 2021CFA014), and Health Commission of Hubei Province of China (NO. ZY2021Z005).

Appendix A. Supplementary data

Supplementary data to this article can be found online at https://doi.org/10.1016/j.heliyon.2023.e20145.

References

[1] T. Kietzmann, Metabolic zonation of the liver: the oxygen gradient revisited, Redox Biol. 11 (2017) 622–630.
[2] M.M. Phipps, et al., Acute liver injury in COVID-19: prevalence and association with clinical outcomes in a large U.S. Cohort, Hepatology 72 (3) (2020) 807–817.
[3] J.P. Sowa, G. Gerken, A. Canbay, Acute liver failure - it's just a matter of cell death, Cell Metabol. 34 (4) (2016) 423–428.
[4] M. Yan, et al., Mechanisms of acetaminophen-induced liver injury and its implications for therapeutic interventions, Redox Biol. 17 (2018) 274–283.
[5] T.Q. de Aguiar Vallim, E.J. Tarling, P.A. Edwards, Pleiotropic roles of bile acids in metabolism, Cell Metabol. 17 (5) (2013) 657–669.
[6] A.L. Ticho, et al., Intestinal absorption of bile acids in health and disease, Compr. Physiol. 10 (1) (2019) 21–56.
[7] Y. Wang, et al., The role of sphingosine 1-phosphate receptor 2 in bile-acid-induced cholangiocyte proliferation and cholestasis-induced liver injury in mice, Hepatology 65 (6) (2017) 2005–2018.
[8] S. Takahashi, et al., Bile acid sequestration reverses liver injury and prevents progression of nonalcoholic steatohepatitis in Western diet-fed mice, J. Biol. Chem. 295 (14) (2020) 4733–4747.
[9] W.X. Ding, M. Li, X.M. Yin, Selective taste of ethanol-induced autophagy for mitochondria and lipid droplets, Autophagy 7 (2) (2011) 248–249.
[10] J.J. Lemasters, Z. Zhong, Mitophagy in hepatocytes: types, initiators and role in adaptive ethanol metabolism, Liver Res 2 (3) (2018) 125–132.
[11] Y. Wang, et al., Targeting the enterohepatic bile acid signaling induces hepatic autophagy via a CYP7A1-AKT-mTOR Axis in mice, Gastroenterol. Hepatol. 3 (2) (2017) 245–260.
[12] X. Du, et al., Impaired hepatic autophagic activity in dairy cows with severe fatty liver is associated with inflammation and reduced liver function, J. Dairy Sci. 101 (12) (2018) 11175–11185.
[13] T. Ueno, M. Komatsu, Autophagy in the liver: functions in health and disease, Nat. Rev. Gastroenterol. Hepatol. 14 (3) (2017) 170–184.
[14] S. Manley, et al., Farnesoid X receptor regulates forkhead Box O3a activation in ethanol-induced autophagy and hepatotoxicity, Redox Biol. 2 (2014) 991–1002.
[15] K.B. Islam, et al., Bile acid is a host factor that regulates the composition of the cecal microbiota in rats, Gastroenterology 141 (5) (2011) 1773–1781.
[16] L. Lv, et al., Lactobacillus Acidophilus LA14 Alleviates Liver Injury, mSystems, 2021, e0038421.
[17] F. Pan, et al., Transcriptome analysis reveals the hepatoprotective mechanism of soybean meal peptides against alcohol-induced acute liver injury mice, Food Chem. Toxicol. 154 (2021), 112353.
[18] X. Li, et al., Effect of Lactobacillus casei on lipid metabolism and intestinal microflora in patients with alcoholic liver injury, Eur. J. Clin. Nutr. 75 (8) (2021) 1227–1236.
[19] M.R. McGill, H. Jaeschke, Animal models of drug-induced liver injury, Biochim. Biophys. Acta, Mol. Basis Dis. 1865 (5) (2019) 1031–1039.
[20] X. Li, et al., Hepatoprotective effect of apolipoprotein A4 against carbon tetrachloride induced acute liver injury through mediating hepatic antioxidant and inflammation response in mice, Biochem. Biophys. Res. Commun. 534 (2021) 659–665.
[21] V. Unsal, M. Cicek, I. Sabancilar, Toxicity of Carbon Tetrachloride, Free Radicals and Role of Antioxidants, Rev Environ Health, 2020.

[22] S. Ali, et al., Protective potential of Parrotiopsis jacquemontiana (Decne) Rehder on carbon tetrachloride induced hepatotoxicity in experimental rats 95 (2017) 1853–1867.
[23] Y. Li, et al., Vine tea (Ampelopsis grossedentata) extract attenuates CCl4 -induced liver injury by restoring gut microbiota dysbiosis in mice, Mol. Nutr. Food Res. (2022), e2100892.
[24] J. Xiang, et al., Dietary supplementation of vine tea ameliorates glucose and lipid metabolic disorder via akt signaling pathway in diabetic rats, Molecules 24 (10) (2019).
[25] J. Chen, et al., Kaempferol alleviates acute alcoholic liver injury in mice by regulating intestinal tight junction proteins and butyrate receptors and transporters, Toxicology 429 (2020), 152338.
[26] X. Zeng, et al., Dihydromyricetin ameliorates nonalcoholic fatty liver disease by improving mitochondrial respiratory capacity and redox homeostasis through modulation of SIRT3 signaling, Antioxidants Redox Signal. 30 (2) (2019) 163–183.
[27] C. Guo, et al., Myricetin ameliorates ethanol-induced lipid accumulation in liver cells by reducing fatty acid biosynthesis, Mol. Nutr. Food Res. 63 (14) (2019), e1801393.
[28] Y. Shen, et al., Myricitrin pretreatment ameliorates mouse liver ischemia reperfusion injury, Int. Immunopharm. 89 (Pt A) (2020), 107005.
[29] Q. Zhang, et al., Recent advances in research on vine tea, a potential and functional herbal tea with dihydromyricetin and myricetin as major bioactive compounds 11 (5) (2021) 555–563.
[30] Y. Geng, et al., The common dietary flavonoid myricetin attenuates liver fibrosis in carbon tetrachloride treated mice 61 (4) (2017), 1600392.
[31] Q.-C. Cheng, et al., Dihydromyricetin ameliorates chronic liver injury by reducing pyroptosis 26 (41) (2020) 6346.
[32] Y.K. Lee, J.A. Lee, Role of the mammalian ATG8/LC3 family in autophagy: differential and compensatory roles in the spatiotemporal regulation of autophagy, BMB Rep 49 (8) (2016) 424–430.
[33] Z. Deng, et al., ALS-FTLD-linked mutations of SQSTM1/p62 disrupt selective autophagy and NFE2L2/NRF2 anti-oxidative stress pathway, Autophagy 16 (5) (2020) 917–931.
[34] B. Khambu, et al., Hepatic autophagy deficiency compromises farnesoid X receptor functionality and causes cholestatic injury, Hepatology 69 (5) (2019) 2196–2213.
[35] Y. Liu, et al., Probiotic Lactobacillus rhamnosus GG prevents liver fibrosis through inhibiting hepatic bile acid synthesis and enhancing bile acid excretion in mice, Hepatology 71 (6) (2020) 2050–2066.
[36] Y. Song, et al., Dihydromyricetin Prevents Obesity via Regulating Bile Acid Metabolism Associated with the Farnesoid X Receptor in Ob/ob Mice, Food Funct, 2022.
[37] Q. Hu, et al., Baicalin and the liver-gut system: pharmacological bases explaining its therapeutic effects, Pharmacol. Res. 165 (2021), 105444.
[38] M. Ali, et al., Selected hepatoprotective herbal medicines: Evidence from ethnomedicinal applications, animal models, and possible mechanism of actions 32 (2) (2018) 199–215.
[39] H.-J. Lin, et al., Hepatoprotective effects of Yi Guan Jian, an herbal medicine, in rats with dimethylnitrosamine-induced liver fibrosis 134 (3) (2011) 953–960.
[40] D.-Y. Lee, et al., Dietary Curcumin Attenuates Hepatic Cellular Senescence by Suppressing the MAPK/NF-κB Signaling Pathway in Aged Mice 12 (6) (2023) 1165.
[41] W.X. Ding, S. Manley, H.M. Ni, The emerging role of autophagy in alcoholic liver disease, Exp Biol Med 236 (5) (2011) 546–556.
[42] L. Yang, et al., Defective hepatic autophagy in obesity promotes ER stress and causes insulin resistance, Cell Metabol. 11 (6) (2010) 467–478.
[43] N. Mizushima, T. Yoshimori, How to interpret LC3 immunoblotting, Autophagy 3 (6) (2007) 542–545.
[44] S.J. Jeong, et al., p62/SQSTM1 and selective autophagy in cardiometabolic diseases, Antioxidants Redox Signal. 31 (6) (2019) 458–471.
[45] S. Manley, J.A. Williams, W.X. Ding, Role of p62/SQSTM1 in liver physiology and pathogenesis, Exp Biol Med 238 (5) (2013) 525–538.
[46] Z.-y. Zhang, et al., Dihydromyricetin Alleviates H9C2 Cell Apoptosis and Autophagy by Regulating CircHIPK3 Expression and PI3K/AKT/mTOR Pathway 29 (5) (2023) 434–440.
[47] J. Zhang, et al., Synergistic effect of cucurbitacin E and myricetin on Anti-Non-Small cell lung cancer: Molecular mechanism and therapeutic potential 111 (2023), 154619.
[48] D. Bing-Xin, L. Pei, L.J.C.J.o.N.M. Jun, EGCG and ECG induce apoptosis and decrease autophagy via the AMPK/mTOR and PI3K/AKT/mTOR pathway in human melanoma cells 20 (4) (2022) 290–300.
[49] J.M. Lee, et al., Nutrient-sensing nuclear receptors coordinate autophagy, Nature 516 (7529) (2014) 112–115.
[50] H. Qian, et al., Autophagy in liver diseases: a review, Mol Aspects Med (2021), 100973.
[51] A. Perino, et al., Molecular physiology of bile acid signaling in health, disease, and aging, Physiol. Rev. 101 (2) (2021) 683–731.
[52] S. Seok, et al., Transcriptional regulation of autophagy by an FXR-CREB axis, Nature 516 (7529) (2014) 108–111.
[53] S.I. Sayin, et al., Gut microbiota regulates bile acid metabolism by reducing the levels of tauro-beta-muricholic acid, a naturally occurring FXR antagonist, Cell Metabol. 17 (2) (2013) 225–235.
[54] J.Y.L. Chiang, J.M. Ferrell, Bile acids as metabolic regulators and nutrient sensors, Annu. Rev. Nutr. 39 (2019) 175–200.
[55] P.K. Martin, K. Cadwell, Regulation of interferon signaling in response to gut microbes by autophagy, Gut Microb. 11 (1) (2020) 126–134.
[56] Y. Song, et al., Dihydromyricetin prevents obesity via regulating bile acid metabolism associated with the farnesoid X receptor in ob/ob mice, Food Funct. 13 (5) (2022) 2491–2503.
[57] M. Juarez-Fernandez, et al., The synbiotic combination of akkermansia muciniphila and quercetin ameliorates early obesity and NAFLD through gut microbiota reshaping and bile acid metabolism modulation, Antioxidants 10 (12) (2021).
[58] Y. Lu, et al., Kaempferol attenuates nonalcoholic steatohepatitis by regulating serum and liver bile acid metabolism, Front. Pharmacol. 13 (2022), 946360.
[59] S. Rakoff-Nahoum, et al., Recognition of commensal microflora by toll-like receptors is required for intestinal homeostasis, Cell 118 (2) (2004) 229–241.
[60] Z. Wang, et al., Gut flora metabolism of phosphatidylcholine promotes cardiovascular disease, Nature 472 (7341) (2011) 57–63.
[61] X. Zhang, et al., Chitosan oligosaccharides attenuate loperamide-induced constipation through regulation of gut microbiota in mice, Carbohydr. Polym. 253 (2021), 117218.
[62] L. Huang, et al., 5-Aminosalicylic acid ameliorates dextran sulfate sodium-induced colitis in mice by modulating gut microbiota and bile acid metabolism, Cell. Mol. Life Sci. 79 (8) (2022) 460.